

Grip as Needed, Glide on Demand: Ultrasonic Lubrication for Robotic Locomotion

Mostafa A. Atalla^{1,2,*}, Daan van Bemmel¹, Jack Cummings¹,
Paul Breedveld¹, Michaël Wiertlewski^{2,†}, and Aimée Sakes^{1,†}

Abstract—Friction is the essential mediator of terrestrial locomotion, yet in robotic systems it is almost always treated as a passive property fixed by surface materials and conditions. Here, we introduce ultrasonic lubrication as a method to actively control friction in robotic locomotion. By exciting resonant structures at ultrasonic frequencies, contact interfaces can dynamically switch between "grip" and "slip" states, enabling locomotion. We developed two friction control modules, a cylindrical design for lumen-like environments and a flat-plate design for external surfaces, and integrated them into bio-inspired systems modeled after inchworm and wasp ovipositor locomotion. Both systems achieved bidirectional locomotion with nearly perfect locomotion efficiencies that exceeded 90%. Friction characterization experiments further demonstrated substantial friction reduction across various surfaces, including rigid, soft, granular, and biological tissue interfaces, under dry and wet conditions, and on surfaces with different levels of roughness, confirming the broad applicability of ultrasonic lubrication to locomotion tasks. These findings establish ultrasonic lubrication as a viable active friction control mechanism for robotic locomotion, with the potential to reduce design complexity and improve efficiency of robotic locomotion systems.

I. INTRODUCTION

Biological organisms achieve remarkable locomotion by exploiting frictional interactions at the body–environment interface. Inchworms advance using sequential anchoring of body segments and extension–contraction cycles, while earthworms employ retrograde peristaltic waves aided by ventral setae to modulate grip along the body [1], [2], [3], [4]. Parasitic wasps, in contrast, steer ultra-thin ovipositors through dense substrates via reciprocating, interlocking valves (sliders) that create directional friction asymmetry, enabling tissue penetration without buckling [5], [6], [7]. These natural strategies illustrate recurring principles of locomotion that rely on regulating contact pressure, creating friction anisotropy, or coordinating imbalances in anchoring and sliding elements.

Such principles have inspired a wide range of robotic devices designed for operation in confined or challenging environments. Worm-like and inchworm-inspired designs have been developed for search-and-rescue in rubble and collapsed structures, for in-pipe inspection in industrial

settings, and for minimally invasive medical procedures such as gastrointestinal endoscopy [8], [9], [10], [11], [12], [13], [14]. Representative platforms include peristaltic soft crawlers for cluttered terrain, modular inchworm robots with alternating anchors, and worm-like in-pipe robots that conform to varying diameters while maintaining traction [2], [15], [16]. In gastrointestinal endoscopy specifically, multiple reviews highlight bio-inspired locomotion strategies and discuss translational challenges such as mucosal safety, navigation, and tether constraints [12], [13], [14].

Across these developments, researchers have sought to control locomotion primarily through modulation of the normal force at the interface, engineering of anisotropic surface features, or creating friction asymmetry by keeping more elements stationary than moving during each phase of the gait. Inflatable or variable-stiffness structures, for example, regulate normal force to alternately anchor and release body segments, simplifying gait timing in cluttered environments [17], [18]. Direction-dependent pads, bristles, or scale-like features create anisotropic surfaces that slide easily forward but resist backward motion [19], [20], [21], [3]. Inchworm and ovipositor-inspired designs instead vary how many contacts are fixed versus sliding during each cycle, biasing net displacement [15], [6], [5]. While effective, these methods depend strongly on surface texture, lose performance on wet or compliant substrates, limiting adaptability in heterogeneous environments.

In this paper, we introduce ultrasonic lubrication, also known as ultrasonic friction modulation, as a new paradigm for friction control in robotic locomotion. Unlike existing approaches that alter contact pressure or exploit structural anisotropy, ultrasonic lubrication acts directly on the coefficient of friction by generating a thin, pressurized fluid film at the interface. By dynamically adjusting the coefficient of friction with the environment, a locomotor can determine when and where to grip or slip, moving beyond the constraints of passive materials. This perspective suggests opportunities not only to improve the efficiency of established locomotion strategies, such as inchworm gaits, but also to enable entirely new locomotion modes. For example, whereas conventional reciprocating ovipositor-inspired systems typically require three or more contact elements to generate directional asymmetry, ultrasonic lubrication can potentially offer the possibility of reducing this requirement, thereby simplifying mechanical design. To investigate these opportunities, we present two designs for friction control modules using the principle of ultrasonic lubrication, and

[†]These authors share last authorship

¹M. A. Atalla, D. van Bemmel, J. Cummings, P. Breedveld, and A. Sakes are with the Department of BioMechanical Engineering, Delft University of Technology (TU Delft), 2628 CD Delft, The Netherlands.

²M. A. Atalla and M. Wiertlewski are with the Department of Cognitive Robotics, Delft University of Technology (TU Delft), 2628 CD Delft, The Netherlands.

*Corresponding author: m.a.a.atalla@tudelft.nl

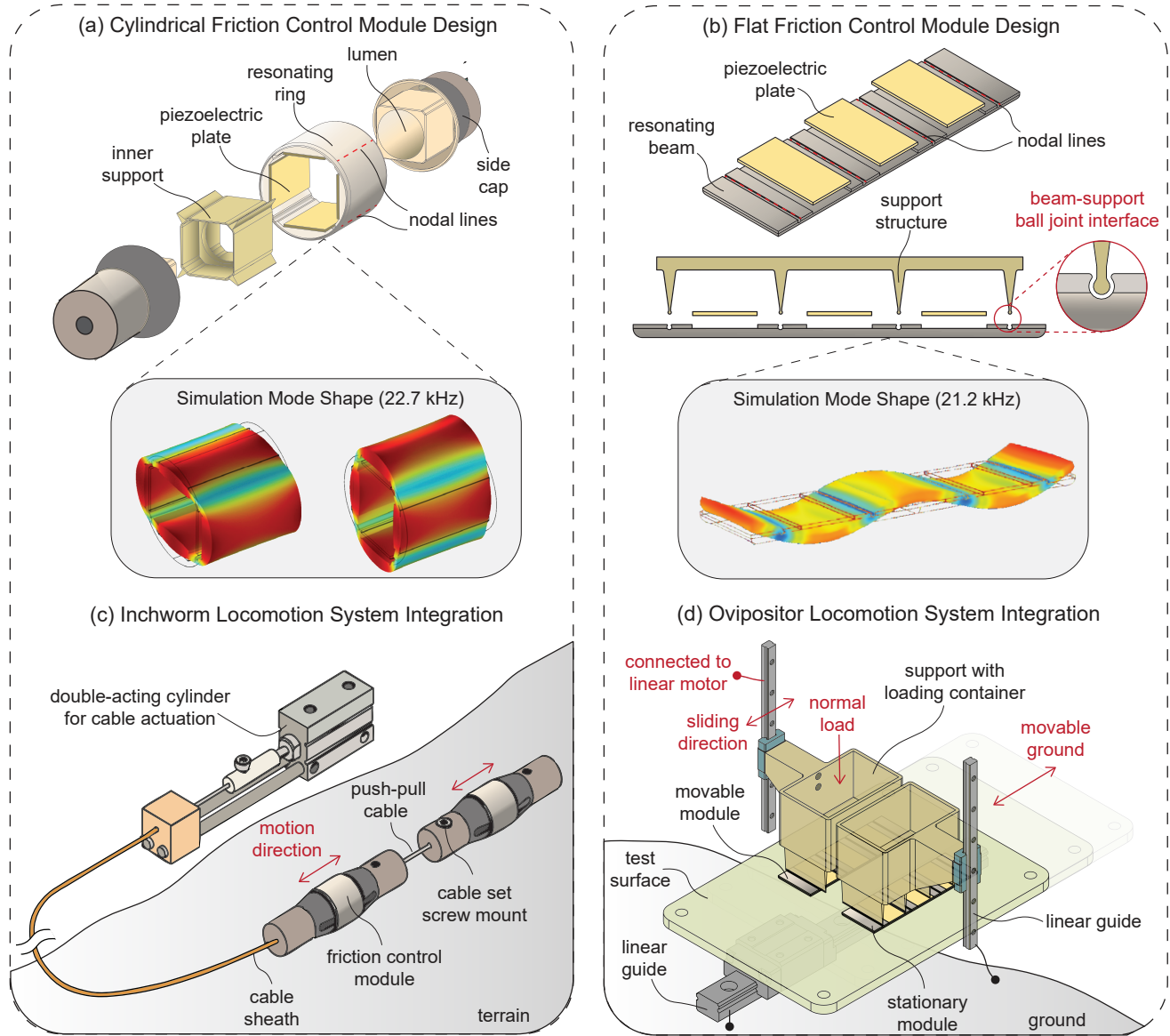


Fig. 1. **Design and integration of cylindrical and flat friction control modules for bio-inspired locomotion.** (a) Cylindrical module: a 10 mm ring-shaped resonator with four bonded piezoelectric plates, supported at nodal lines by an internal frame to minimize interference with oscillation. Finite element analysis confirmed operation in the second flexural mode at 22.7 kHz. (b) Flat module: a $32 \times 10 \times 1$ mm slider resonator with piezoelectric plates bonded at antinodes and supported via a ball-joint groove at nodal lines. Simulation results predicted the third flexural mode at 21.2 kHz. (c) Inchworm-inspired locomotion system: two cylindrical modules connected by a push-pull cable-sheath mechanism and actuated by a double-acting cylinder, enabling bidirectional motion through selective activation of each module. (d) Ovipositor-inspired locomotion system: two flat modules, one fixed and one mounted to a linear actuator, enabling bidirectional motion through selective activation of the movable module during the motion cycle.

demonstrate their integration into example bio-inspired locomotion systems. Through these examples, we assess the viability of ultrasonic lubrication for locomotion and explore its potential to extend beyond biological strategies toward more efficient locomotion.

In the remainder of this paper, Section II introduces the working principle of ultrasonic lubrication. Section III presents the design, fabrication, and integration of two friction control modules. Section IV describes the experimental setup and protocols, and Section V reports the vibration, locomotion, and friction modulation results. Finally, Section VI summarizes the findings and discusses their implications for

future robotic locomotion systems.

II. WORKING PRINCIPLE

A. Ultrasonic Lubrication

When two solid bodies come into contact and slide against each other, friction emerges due to the interaction of a limited number of microscopic surface asperities. These asperities form junctions with the opposing surface, creating the real contact area, which is much smaller than the nominal or apparent area of contact. As a result, a large fraction of the apparent contact region does not engage directly,

allowing surrounding fluid to become trapped and form a thin interfacial layer, commonly referred to as a squeeze film.

Introducing transverse ultrasonic vibrations to one of the contacting bodies causes the trapped fluid to undergo non-linear compression, generating an excess pressure within the fluid film. This additional pressure pushes the two surfaces apart and produces a tunable coefficient of friction. This mechanism, known as ultrasonic lubrication or ultrasonic friction modulation [22], [23], directly links the degree of separation to the vibration amplitude, enabling precise and active control of lubrication at the interface [22].

Ultrasonic lubrication has been successfully applied in a range of contexts where friction control is critical, including tactile displays [24], non-contact object manipulation [25], and squeeze-film bearings [26], [27]. Furthermore, it has been shown to operate effectively in submerged liquid environments [28], performing comparably to its use in air, which highlights its adaptability to diverse operating conditions. This ability to switch smoothly between high- and low-friction states across different environments points to its promise for applications requiring active friction modulation, such as in catheters [29].

B. Biological Locomotion Use Cases

To investigate the potential of ultrasonic lubrication as a means of active friction control for locomotion, we examined two representative biological strategies that exemplify complementary modes of movement. The first is inchworm locomotion, which operates through sequential anchoring and advancement of body segments. The second is peristaltic slider locomotion, exemplified by the wasp ovipositor, which relies on the reciprocating sliding of multiple valves. These two cases were selected because they are both widespread in nature and have inspired numerous robotic designs, making them well-suited as biological benchmarks for proof-of-concept demonstrations.

The inchworm achieves locomotion through discrete phases of anchoring and advancing. It alternately grips the substrate with its front and rear prolegs, contracts its body to bring the rear forward, then extends again to project the front forward. At each stage of the cycle, one part of the body remains fixed while the other is repositioned, ensuring directional progress. This stop-and-go strategy produces net displacement without requiring continuous wave propagation and has inspired a range of robotic implementations, often termed “inchworm robots” or “two-anchor crawlers,” where alternating anchoring is realized with frictional pads, clamps, or suction elements.

Parasitic wasps achieve locomotion of their ovipositor through a peristaltic slider mechanism, where three slender valves—one dorsal and two ventral—are held together by a tongue-and-groove connection that constrains them radially while permitting longitudinal sliding. During penetration, locomotion is generated by sequential reciprocation: while one valve advances forward into the substrate, the other two remain stationary and provide anchoring through friction, counteracting the penetrating force. The advancing valve then

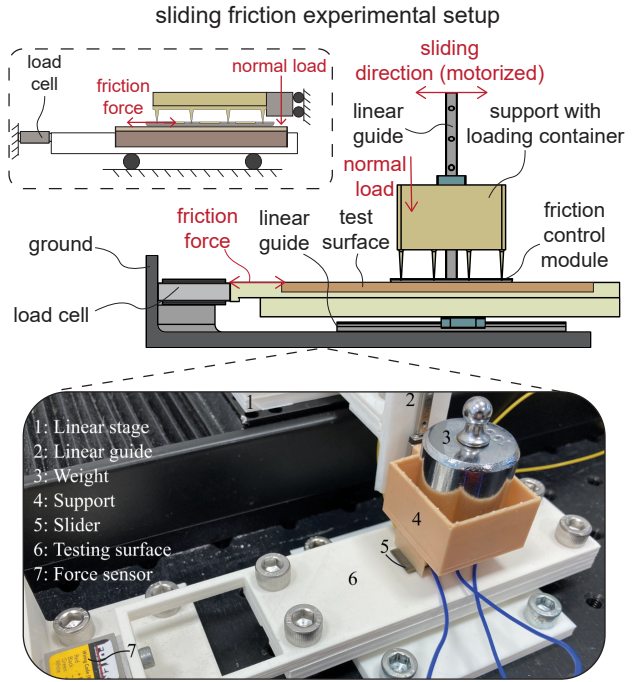


Fig. 2. **Experimental setup for the friction characterization experiments.** A miniature load cell mounted along the sliding axis measured friction forces via a bracket guided on a horizontal stage, while the slider was mounted to a vertical linear guide for motorized horizontal motion and free vertical displacement. A 100 g weight (≈ 1 N) provided the normal load. Two protocols were tested: (i) sliding with and without continuous vibration at 280 V to assess sustained lubrication, and (ii) sliding with the excitation voltage ramped from 0 to 280 V to evaluate dynamic friction modulation. Tests were performed on dry and wet PLA, sandpapers of different grit sizes, granular soil, and ex-vivo porcine intestinal tissue.

becomes stationary while another valve moves forward, and this cycle repeats across all three valves. After each has advanced in turn, the valves reset in unison, producing a net forward displacement of the ovipositor. By iterating this cycle, the ovipositor is able to steadily penetrate deep into host tissue or other substrates with minimal overall insertion force.

III. DESIGN & IMPLEMENTATION

A. Conceptual Design

To implement the two locomotion strategies using ultrasonic lubrication, the first step is the development of a friction control module, which serves as the fundamental unit of the locomotion system. We present two module designs: a cylindrical block intended for locomotion within lumens (internal locomotion) and a flat-plate block designed for locomotion on external surfaces. For ultrasonic lubrication to be effective, each module must be capable of producing vibration amplitudes of at least $2 \mu\text{m}$ at ultrasonic frequencies of 20 kHz or higher [30], [31].

Both modules share a common design principle. The resonating structure is engineered to exhibit a preferred flexural resonance mode in the ultrasonic range. Piezoelectric plates are positioned at the antinodes of this mode so that, when activated, they excite the target resonance and

amplify vibration across the structure. To minimize energy loss, structural supports are positioned at nodal lines, where displacement is nearly zero. These supports, implemented through grooves and needle-like contact elements, allow free rotation at the nodes and thus reduce interference with vibration. This approach enables the resonating structure to act as a mechanical amplifier, achieving the vibration amplitudes required for effective ultrasonic lubrication (Fig. 1(a)(b)).

Cylindrical Friction Control Module Design

The cylindrical module consists of a ring-shaped resonator with four bonded piezoelectric plates, designed to operate in its second flexural resonance mode, as illustrated in Fig. 1(a). The prototype used for characterization had an outer diameter of 10 mm, following the design of [29]. The ring is supported internally by a frame with needle-like edges contacting the resonator at nodal lines. This configuration ensures stability while minimizing interference with oscillation. Finite element analysis, using stainless steel as material, predicted a resonance frequency of 22.7 kHz and a maximum vibration amplitude of approximately 4 μm per 100 V excitation.

Flat Friction Control Module Design

The flat module is a rectangular slider resonator ($32 \times 10 \times 1$ mm) with three piezoelectric plates bonded at the antinodes, designed to operate in its third flexural mode, as shown in Fig. 1(b). The slider is supported at its nodal lines through small circular cutouts that accommodate a ball-joint groove and thin-legged supports, constraining the structure while allowing free rotation. This configuration ensures stability while minimizing interference with oscillation. Finite element analysis, using stainless steel as the material, predicted a resonance frequency of 21.2 kHz and a maximum vibration amplitude of approximately 4.73 μm .

Prototype Development

Friction control modules, both flat and cylindrical, were fabricated from stainless steel 316 using electrical discharge machining (EDM). Piezoelectric plates (SM112, SteminC, FL, USA) were cut to size and bonded into pre-designed slots with a two-component, electrically insulating adhesive (3M Scotch-Weld Epoxy Structural Adhesive DP490). Each plate included two electrodes on one side, with the back electrode bonded to the resonator surface. Wires were soldered to the exposed electrodes and arranged so that consecutive plates were driven with a phase shift 180°, ensuring excitation of the target resonance mode. The support structures were produced using a stereolithography (SLA) 3D printer (Formlabs, USA), providing the precision required for the fine support legs interfacing with the resonating structures.

Locomotion System Integration

The inchworm-inspired locomotion system was realized using two cylindrical friction control modules with an extensor element positioned between them, as illustrated in Fig. 1(c). The extensor was implemented through a push–pull cable-sheath mechanism, in which the sheath was anchored

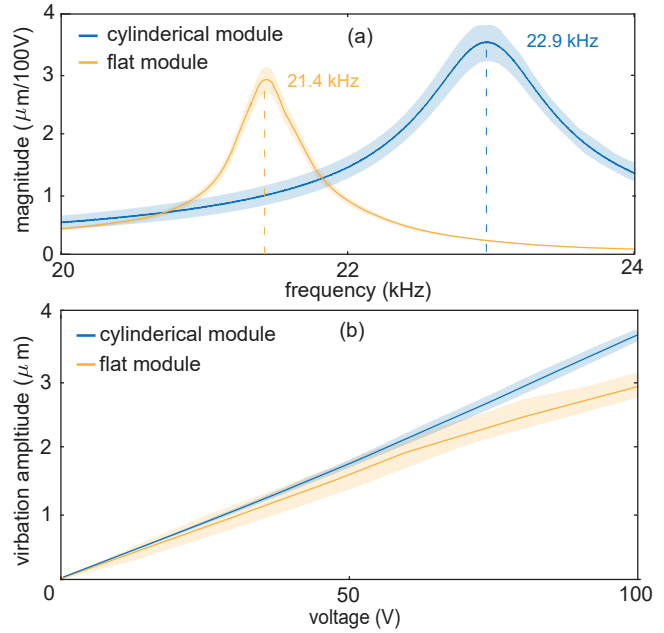


Fig. 3. **Vibration characterization of cylindrical and flat modules.** (a) Frequency response showing resonance peaks at 22.9 kHz for the cylindrical module and 21.4 kHz for the flat module. (b) Vibration amplitude as a function of applied voltage, exhibiting linear growth up to the $\sim 4 \mu\text{m}$ measurement limit of the . Both modules achieved amplitudes exceeding 2 μm at ultrasonic frequencies (≥ 20 kHz), meeting design requirements for ultrasonic lubrication.

to the first module while the inner cable passed through and was fixed to the second module. The push–pull assembly was driven by a double-acting linear cylinder that actuated the extension and contraction. A computer-programmed control system coordinated the actuation sequence by selectively activating each friction control module based on the desired direction of motion and the phase of the motion cycle.

The ovipositor-inspired locomotion system was constructed using two flat friction control modules, as illustrated in Fig. 1(d). One module was fixed in place, while the other was mounted to a linear actuator that provided reciprocating motion. A computer-programmed control system was then used to selectively switch the vibrations of the moving slider on or off, depending on the desired direction of motion and the phase of the motion cycle. This configuration, one fixed and one moving slider, was chosen to simplify implementation: achieving the biological motion cycle with two adjacent sliders would otherwise require independent transmission mechanisms for each, introducing unnecessary design complexity without being central to the goals of this work. By fixing one slider and actuating the other, while allowing the contacting ground surface to slide freely, the same principle of ovipositor locomotion could be demonstrated in a simpler and functionally equivalent manner.

IV. EXPERIMENTAL EVALUATION

To validate the concept of the friction control modules and characterize their performance, we conducted three experiments. The first experiment aimed to characterize and

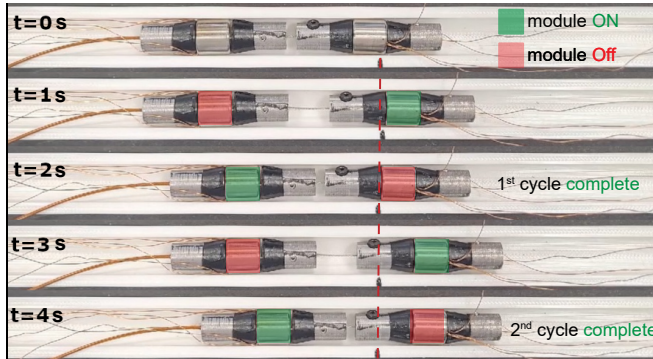


Fig. 4. Time-lapse sequence of the inchworm locomotion system traversing a rigid PLA track. By selectively activating ultrasonic lubrication at each friction control module, forward propulsion is achieved following the inchworm motion cycle. Images are shown at one-second intervals. Refer to supplementary videos 1 & 2 for the demonstration of the use cases presented in this paper including the inchworm locomotion case.

validate the vibration performance of individual modules. The second was a proof-of-concept experiment to demonstrate locomotion enabled by ultrasonic lubrication in both bio-inspired designs, and quantify the resulting locomotion efficiency. The third aimed to assess the ability of the modules to modulate friction across surfaces with different materials and properties.

A. Vibration Characterization Experiment

The resonance properties of the friction control modules were evaluated by measuring the frequency of resonance and the amplitude of the vibration through two complementary tests. First, a frequency response measurement was used to identify the resonant frequency. Second, a voltage sweep was performed at this frequency to quantify the vibration amplitude as a function of the input voltage. Both unsupported and supported sliders were tested to assess the influence of the support structure and each experiment was repeated six times.

The vibration response was measured using a laser Doppler vibrometer (Polytec OFV-5000 Vibrometer Controller). The Laser Doppler Vibrometer tracked the velocity of a marked anti-nodal point at the center of the slider, while the prototypes were powered by a piezo amplifier (Piezo-Drive PD200X4 Voltage Amplifier). The Laser Doppler Vibrometer and amplifier were connected to a data acquisition system (National Instruments USB X Series Multifunction DAQ), which interfaced with a PC for control and data logging.

For the frequency response test, the modules were activated, and the excitation frequency was swept from 20 to 24 kHz at maximum voltage to determine the resonant frequency. For the amplitude test, the frequency was fixed at the identified resonance, and the input voltage was increased from 0 to 100 V in steps of 10 V to record the corresponding vibration amplitudes.

B. Proof-of-concept Locomotion Experiment

We tested both locomotion systems on rigid 3D-printed PLA substrates to demonstrate the viability of ultrasonic lubrication for locomotion, and to quantify locomotion efficiency. The inchworm-inspired system was evaluated on a semi-cylindrical substrate matching the geometry of its cylindrical friction control modules, while the ovipositor-inspired system was tested on a flat substrate. Each system was first actuated without ultrasonic lubrication to establish a baseline, after which the same motion sequence was repeated with lubrication activated. For each test, the distance traveled by the system was measured and divided by the actuator stroke—the theoretical displacement without friction—to determine locomotion efficiency.

C. Friction Characterization Experiment

Following the proof-of-concept, we conducted sliding friction experiments using only the flat friction control module to evaluate the slider's ability to modulate friction across a range of surface environments: a rigid 3D-printed PLA surface under both dry and wet conditions, a granular soil surface, and surfaces with varying roughness using coarse (150 grit) and fine (240 grit) sandpapers. Finally, we performed tests on wet ex-vivo biological tissue (porcine intestinal tissue) to explore the potential for medical applications.

Friction forces were measured with a miniature load cell (Futek LSB200) mounted along the sliding axis and connected to the test surface through a mounting bracket, which was supported by a horizontal linear guide (IKO Nippon Thompson LWLC3C1R60T0H, LWL) to allow free motion in the direction of the friction force, as illustrated in Fig.2. The slider was attached to a linear actuator (Thorlabs NRT150/M) through a vertical linear guide, providing controlled horizontal displacement while allowing free vertical motion of the slider for mass-based normal loading. The mounting bracket included provisions for additional weights, enabling precise control of the applied normal load.

In this experiment, two sets of tests were conducted. In the first, the friction control module was loaded with a 100 g weight (≈ 1 N normal load) and driven forward and backward over a 10 mm distance at 1 mm/s. The test was performed first without vibrations and then with continuous activation at 280 V to evaluate the sustainability of the lubrication effect under steady excitation. In the second set of trials, the module's ability to modulate friction was assessed by sliding it over a 15 mm distance at 1 mm/s under the same 1 N load while gradually ramping the input voltage from 0 to 280 V. Vibrations were activated after 5 s, and the voltage was increased linearly to its maximum over the following 5 s, enabling the corresponding change in friction force to be recorded. To quantify the slider's friction modulation capability, we used the friction reduction percentage, which was calculated as follows:

$$\text{friction reduction} = \frac{\mu_{\text{off}} - \mu_{\text{on}}}{\mu_{\text{off}}} \quad (1)$$

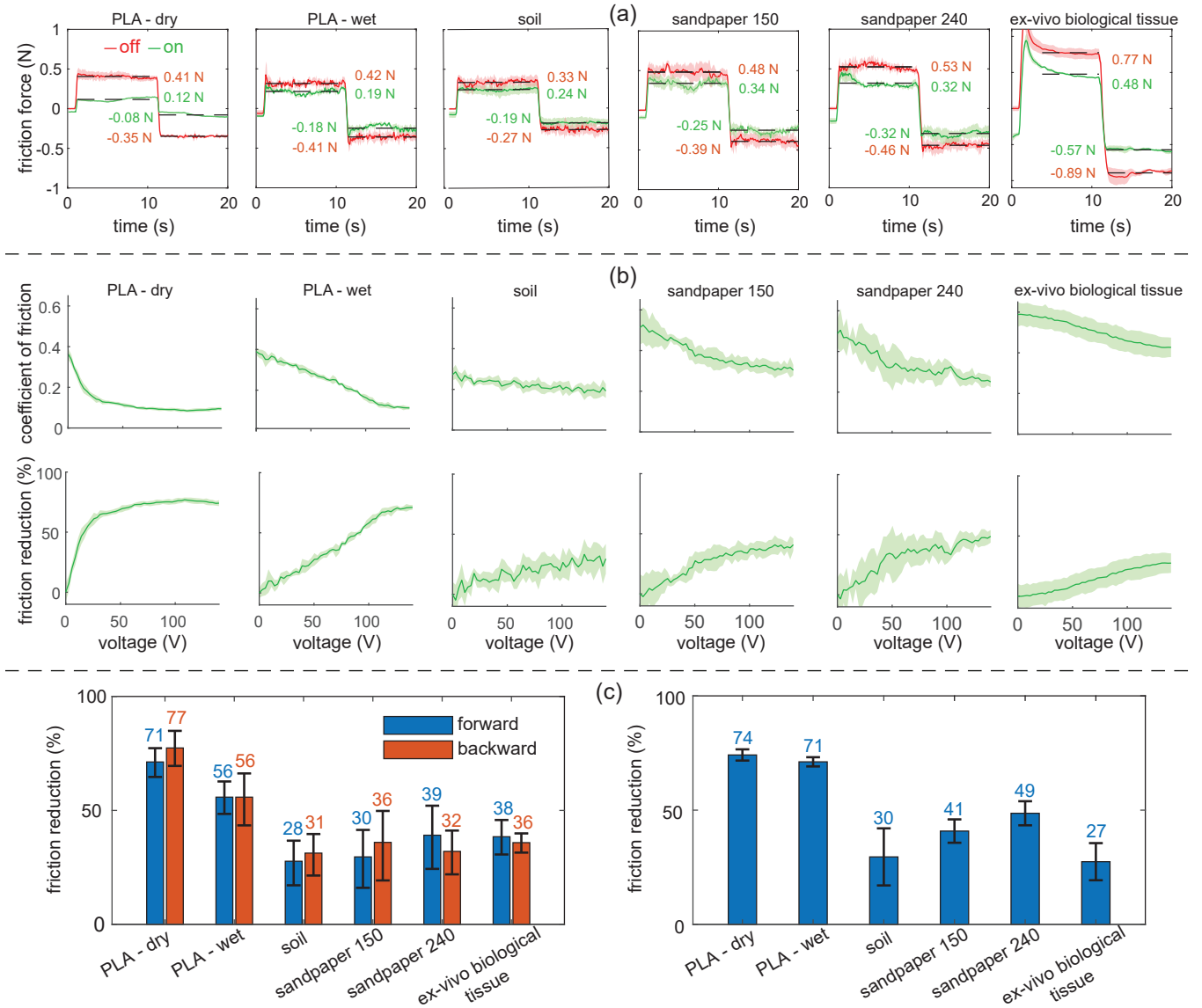


Fig. 5. **Friction modulation experiments across a range of surfaces.** (a) Measured friction forces under forward and backward sliding show that the vibrating slider effectively reduces friction on PLA (dry and wet), soil, sandpaper, and biological tissue (colon). (b) Voltage modulation of coefficient of friction (top row) and corresponding friction reduction percentage (bottom row). On PLA, reduction is consistent with air squeeze-film formation and exhibits nonlinear saturation. Sandpaper surfaces show higher reduction for finer grit (240) compared to coarser grit (150), due to enhanced squeeze-film effects in smaller asperities. Soil produced relatively low reduction owing to its unstable granular contact. On wet PLA with olive oil, viscous adhesion increased friction but ultrasonic vibration still enabled reduction via liquid squeeze-film formation. On colon tissue, viscoelasticity damped vibration energy, limiting reduction. (c) Summary of friction reduction for different substrates during forward-backward sliding (left) and voltage modulation (right) experiments. On pig colon tissue, the slider achieved friction reduction of approximately 37% and 27%, respectively, indicating potential for enhancing the locomotion efficiency of sliding robotic medical devices.

The term μ_{off} represents the average friction experienced by the slider in the non-vibrating case, while μ_{on} represents the average friction in the vibrating case.

V. RESULTS AND DISCUSSION

The vibration characterization experiments revealed the resonance properties of both module types. The cylindrical ring prototype resonated at 22.9 kHz and produced a vibration amplitude of $\approx 3.7 \mu\text{m}/100\text{V}$. The flat slider prototype resonated at 21.4 kHz (Fig. 3(a)) with an amplitude of $\approx 3 \mu\text{m}/100\text{V}$. In both cases, the vibration amplitude increased approximately linearly with driving voltage (Fig. 3(b)) and

reached $\approx 4 \mu\text{m}$ before saturating due to the Laser Doppler Vibrometer measurement limit, indicating that the actual amplitudes at higher voltages are likely higher. These results confirm that both modules meet the ultrasonic lubrication design requirements, producing amplitudes greater than $2 \mu\text{m}$ at ultrasonic frequencies ($\geq 20 \text{ kHz}$).

In the proof-of-concept locomotion experiments, both systems achieved locomotion only when ultrasonic lubrication was activated (Fig. 4), and failed to move in its absence. Without ultrasonic lubrication, the two friction-control modules experienced symmetric friction and therefore generated

no net traction over a cycle. Activating ultrasonic lubrication selectively reduced friction at one module, allowing it to slide while the other remained stationary due to its high friction state. This selective friction control broke the frictional symmetry of the modules, creating the asymmetry required for locomotion. In both systems, bi-directional locomotion was obtained simply by reversing the ultrasonic lubrication activation sequence on the modules (see supplementary videos 1 & 2). The inchworm-inspired system achieved a mean locomotion efficiency of 94.75%, and the ovipositor-inspired system achieved 93.2%. These locomotion efficiencies are specific to the experimental setup and normal loading conditions; however, they demonstrate the potential of ultrasonic lubrication as a friction-control mechanism to reliably generate and switch locomotion.

The sliding friction experiments demonstrated the viability of ultrasonic lubrication across a range of surfaces (Fig. 5), achieving average friction reductions of 71–77% on dry PLA, ≈ 56%–71% on wet PLA, 28–49% on soil and sandpaper, and ≈ 27–38% on *ex-vivo* biological tissue. In the steady-sliding experiments (Fig. 5(a)), the flat friction-control module was first slid forward and backward on each surface without activating ultrasonic lubrication to establish the baseline friction forces. The same forward–backward sliding cycles were then repeated with the ultrasonic lubrication activated. In all cases, activating ultrasonic lubrication reduced the measured friction forces compared to the baseline case, and the reduction remained stable over the forward and backward cycles. This shows that ultrasonic lubrication can provide a steady and consistent direction-independent reduction in friction, rather than a transient effect.

The friction modulation experiments (Fig. 5(b)) further showed that the ultrasonic lubrication effect is controllable beyond the on–off case. Here, ultrasonic lubrication was modulated by modulating the input voltage (and therefore the vibration amplitude) which modulated the coefficient of friction accordingly. As shown in Fig. 5(b), voltage modulation showed a controllable range of the coefficient of friction across all surfaces, demonstrating the ability of ultrasonic lubrication to tune friction continuously by simply adjusting the vibration level.

The friction reduction levels and trends across the different substrates help explain the underlying differences in performance, as summarized in Fig. 5(c) for both the steady-sliding comparison (left) and the voltage-modulation case (right). On smooth dry PLA, the reduction is consistent with the formation of an air squeeze film. Because air is compressible, the film thickness develops nonlinearly with excitation and eventually saturates, which matches the nonlinear trend observed in the voltage modulation experiments. On wet PLA, baseline friction forces were higher due to viscous capillary adhesion; however, ultrasonic lubrication was still able to reduce friction via the formation of a pressurized liquid squeeze film. Unlike air, liquids are nearly incompressible, and vibrations generate squeeze-film pressure mainly through liquid inertia [28], leading to a more linear voltage–friction response compared to air, as shown in Fig. 5(b).

When tested on rough surfaces, the degree of reduction depended on surface roughness. On sandpaper, the finer grit (240) produced slightly greater friction reduction than the coarser grit (150), as the smaller asperities and voids in the finer grit case help to promote stronger squeeze-film formation, resulting in improved lubrication effect. Soil yielded relatively low friction reduction, which can be explained by its granular structure, which creates a constantly changing and non-uniform contact interface, disrupting stable squeeze-film formation, and thus limiting the effect of ultrasonic lubrication. Finally, the *ex-vivo* porcine intestinal tissue interface showed a reduced effect of ultrasonic lubrication compared to that of the rigid wet PLA case, which can be attributed to the viscoelastic properties of tissue. The viscoelasticity of the tissue dissipates part of the vibration energy, which limits the pressure buildup in the squeeze film and thus reduces the lubrication effect.

VI. CONCLUSION

In this work, we introduced ultrasonic lubrication as a friction-control mechanism for robotic locomotion. We presented two friction control module designs, cylindrical and flat, and integrated them into two locomotion systems inspired by inchworm and parasitic wasp ovipositor motion. Vibrometry experiments confirmed that both modules can generate amplitudes exceeding 2 μm at ultrasonic frequencies around 22 kHz, fulfilling the requirements of ultrasonic lubrication. In proof-of-concept locomotion experiments, ultrasonic lubrication enabled bi-directional locomotion in both the inchworm-inspired and ovipositor-inspired systems, with mean efficiencies of 94.75% and 93.2%, while no locomotion was achieved when ultrasonic lubrication was not activated due to friction symmetry. Sliding friction experiments demonstrated the ability of ultrasonic lubrication to achieve stable and tunable friction reduction across a variety of rigid and soft interfaces in dry and wet conditions, highlighting the versatility of ultrasonic lubrication for robotic locomotion applications.

In future work, we will focus on modeling the dynamics of ultrasonic lubrication in locomotion, with particular attention to activation timing during the gait cycle. By relating activation phases to locomotion efficiency and stability, we aim to develop optimized friction control strategies for locomotion and explore additional functionalities, such as adaptive steering and interaction with complex environments.

ACKNOWLEDGMENT

The authors would like to thank Remi van Starkenburg, from central workshop of TU Delft (DEMO), for support fabricating the modules and Maurits Pfaff, Cognitive Robotics department of TU Delft, for support integrating the piezoelectric elements.

REFERENCES

- [1] N. Saga, S. Tesen, T. Sato, and J.-Y. Nagase, “Acquisition of earthworm-like movement patterns of many-segmented peristaltic crawling robots,” *International Journal of Advanced Robotic Systems*, vol. 13, no. 5, p. 1729881416657740, 2016.

[2] L. Xu, R. J. Wagner, S. Liu, Q. He, T. Li, W. Pan, Y. Feng, H. Feng, Q. Meng, X. Zou, *et al.*, “Locomotion of an untethered, worm-inspired soft robot driven by a shape-memory alloy skeleton,” *Scientific reports*, vol. 12, no. 1, p. 12392, 2022.

[3] M. Calisti, G. Picardi, and C. Laschi, “Fundamentals of soft robot locomotion,” *Journal of The Royal Society Interface*, vol. 14, no. 130, p. 20170101, 2017.

[4] R. Das, S. P. M. Babu, F. Visentin, S. Palagi, and B. Mazzolai, “An earthworm-like modular soft robot for locomotion in multi-terrain environments,” *Scientific Reports*, vol. 13, no. 1, p. 1571, 2023.

[5] N. M. van Meer, U. Cerkvenik, C. M. Schlepütz, J. L. van Leeuwen, and S. W. Gussekloo, “The ovipositor actuation mechanism of a parasitic wasp and its functional implications,” *Journal of anatomy*, vol. 237, no. 4, pp. 689–703, 2020.

[6] A. Sakes, I. A. Van de Steeg, E. P. De Kater, P. Posthoorn, M. Scali, and P. Breedveld, “Development of a novel wasp-inspired friction-based tissue transportation device,” *Frontiers in Bioengineering and Biotechnology*, vol. 8, p. 575007, 2020.

[7] M. I. Nikelshparg, E. I. Nikelshparg, V. V. Anikin, and A. A. Polilov, “Extraordinary drilling capabilities of the tiny parasitoid eupelmus messene walker (hymenoptera, eupelmidae),” *Journal of Hymenoptera Research*, vol. 96, pp. 715–722, 2023.

[8] M. Kulkarni, S. Edward, T. Golecki, B. Kaehr, and H. Golecki, “Soft robots built for extreme environments,” *Soft Science*, vol. 5, no. 1, pp. N–A, 2025.

[9] A. Sebastian, “Soft robotics for search and rescue: Advancements, challenges, and future directions,” *arXiv preprint arXiv:2502.12373*, 2025.

[10] G. Blewitt, D. Cheneler, J. Andrew, and S. Monk, “A review of worm-like pipe inspection robots: Research, trends and challenges,” *Soft Science*, vol. 4, no. 2, p. 13, 2024.

[11] R. S. Elankavi, D. Dinakaran, R. K. Chetty, M. Ramya, and D. H. Samuel, “A review on wheeled type in-pipe inspection robot,” *International journal of mechanical engineering and robotics research*, vol. 11, no. 10, pp. 745–754, 2022.

[12] J. F. Ahmed, E. Franco, F. R. Y. Baena, A. Darzi, and N. Patel, “A review of bioinspired locomotion in lower gi endoscopy,” *Robotica*, pp. 1–11, 2024.

[13] A. Menciassi and P. Dario, “Bio-inspired solutions for locomotion in the gastrointestinal tract: background and perspectives,” *Philosophical Transactions of the Royal Society of London. Series A: Mathematical, Physical and Engineering Sciences*, vol. 361, no. 1811, pp. 2287–2298, 2003.

[14] G. Ciuti, R. Caliò, D. Camboni, L. Neri, F. Bianchi, A. Arezzo, A. Koulaouzidis, S. Schostek, D. Stoyanov, C. M. Oddo, *et al.*, “Frontiers of robotic endoscopic capsules: a review,” *Journal of micro-bio robotics*, vol. 11, no. 1, pp. 1–18, 2016.

[15] W. Saab, P. Racioppo, A. Kumar, and P. Ben-Tzvi, “Design of a miniature modular inchworm robot with an anisotropic friction skin,” *Robotica*, vol. 37, no. 3, p. 521–538, 2019.

[16] J. Z. Ge, A. A. Calderón, L. Chang, and N. O. Pérez-Arcinbia, “An earthworm-inspired friction-controlled soft robot capable of bidirectional locomotion,” *Bioinspiration & Biomimetics*, vol. 14, no. 3, p. 036004, 2019.

[17] J.-C. Chang, H. Dai, X. Wang, D. Axinte, and X. Dong, “Development of a continuum robot with inflatable stiffness-adjustable elements for in-situ repair of aeroengines,” *Robotics and Computer-Integrated Manufacturing*, vol. 95, p. 103018, 2025.

[18] A. Ataka, T. Abrar, F. Putzu, H. Godaba, and K. Althoefer, “Observer-based control of inflatable robot with variable stiffness,” in *Proceedings of the 2020 IEEE/RSJ International Conference on Intelligent Robots and Systems (IROS)*, (Las Vegas, NV, USA), pp. 8646–8652, IEEE, Oct. 2020.

[19] P. Manoonpong, D. Petersen, A. Kovalev, F. Wörgötter, S. N. Gorb, M. Spinner, and L. Heepe, “Enhanced locomotion efficiency of a bio-inspired walking robot using contact surfaces with frictional anisotropy,” *Scientific reports*, vol. 6, no. 1, p. 39455, 2016.

[20] H. Kim, S. Cho, D. Kam, S. J. Lee, S. Park, D. Choi, and J. Kim, “Tendon-driven crawling robot with programmable anisotropic friction by adjusting out-of-plane curvature,” *Machines*, vol. 11, no. 7, p. 763, 2023.

[21] H. T. Tramsen, S. N. Gorb, H. Zhang, P. Manoonpong, Z. Dai, and L. Heepe, “Inversion of friction anisotropy in a bio-inspired asymmetrically structured surface,” *Journal of The Royal Society Interface*, vol. 15, no. 138, p. 20170629, 2018.

[22] M. Wiertlewski, R. F. Friesen, and J. E. Colgate, “Partial squeeze film levitation modulates fingertip friction,” *Proceedings of the National Academy of Sciences of the United States of America*, vol. 113, no. 33, pp. 9210–9215, 2016.

[23] R. F. Friesen, M. Wiertlewski, M. A. Peshkin, and J. E. Colgate, “The contribution of air to ultrasonic friction reduction,” in *2017 IEEE World Haptics Conference (WHC)*, pp. 517–522, 2017.

[24] L. Winfield, J. Glassmire, J. E. Colgate, and M. Peshkin, “T-PaD: Tactile pattern display through variable friction reduction,” *Proceedings - Second Joint EuroHaptics Conference and Symposium on Haptic Interfaces for Virtual Environment and Teleoperator Systems, World Haptics 2007*, pp. 421–426, 2007.

[25] R. Gabai, R. Shaham, S. Davis, N. Cohen, and I. Bucher, “A Contactless Stage Based on Near-Field Acoustic Levitation for Object Handling and Positioning-Concept, Design, Modeling, and Experiments,” *IEEE/ASME Transactions on Mechatronics*, vol. 24, no. 5, pp. 1954–1963, 2019.

[26] S. Zhao, S. Mojrzisch, and J. Wallaschek, “An ultrasonic levitation journal bearing able to control spindle center position,” *Mechanical Systems and Signal Processing*, vol. 36, no. 1, pp. 168–181, 2013.

[27] M. Shi, K. Feng, J. Hu, J. Zhu, and H. Cui, “Near-field acoustic levitation and applications to bearings: A critical review,” *International Journal of Extreme Manufacturing*, vol. 1, no. 3, 2019.

[28] M. A. Atalla, R. A. J. van Ostayen, A. Sakes, and M. Wiertlewski, “Incompressible squeeze-film levitation,” *Applied Physics Letters*, vol. 122, no. 24, 2023.

[29] M. A. Atalla, J. J. Tuijp, M. Wiertlewski, and A. Sakes, “Toward variable-friction catheters using ultrasonic lubrication,” *IEEE Transactions on Medical Robotics and Bionics*, vol. 6, no. 4, pp. 1375–1381, 2024.

[30] M. Biet, F. Giraud, and B. Lemaire-Semail, “Squeeze film effect for the design of an ultrasonic tactile plate,” *IEEE Transactions on Ultrasonics, Ferroelectrics, and Frequency Control*, vol. 54, no. 12, pp. 2678–2688, 2007.

[31] T. Watanabe and S. Fukui, “A method for controlling tactile sensation of surface roughness using ultrasonic vibration,” in *Proceedings of 1995 IEEE International Conference on Robotics and Automation*, vol. 1, pp. 1134–1139 vol.1, 1995.